J. Math. Biol. (2009) 58:219–233
DOI 10.1007/s00285-008-0193-z

Mathematical Biology

Stochastic modelling of tumour-induced angiogenesis

Vincenzo Capasso · Daniela Morale

Received: 24 July 2007 / Revised: 21 May 2008 / Published online: 10 June 2008

Abstract A major source of complexity in the mathematical modelling of an angiogenic process derives from the strong coupling of the kinetic parameters of the relevant stochastic branching-and-growth of the capillary network with a family of interacting underlying fields. The aim of this paper is to propose a novel mathematical approach for reducing complexity by (locally) averaging the stochastic cell, or vessel densities in the evolution equations of the underlying fields, at the mesoscale, while keeping stochasticity at lower scales, possibly at the level of individual cells or vessels. This method leads to models which are known as hybrid models. In this paper, as a working example, we apply our method to a simplified stochastic geometric model, inspired by the relevant literature, for a spatially distributed angiogenic process. The branching mechanism of blood vessels is modelled as a stochastic marked counting process describing the branching of new tips, while the network of vessels is modelled as the union of the trajectories developed by tips, according to a system of stochastic differential equations à la Langevin.

Keywords Angiogenesis · Stochastic differential equations · Birth and growth processes · Hybrid models

Mathematics Subject Classification (2000) 60G57 · 60H10 · 60H30 · 60B10 · 92B05

V. Capasso (✉) · D. Morale
Department of Mathematics, University of Milan, Milan, Italy
e-mail: vincenzo.capasso@unimi.it

D. Morale
e-mail: daniela.morale@mat.unimi.it

1 Introduction

Angiogenesis, the growth of new blood vessels, is an important natural process occurring in the body, both in health and in disease. It occurs in the healthy body for healing wounds, and for restoring blood flow to tissues after injury or insult. The healthy body controls angiogenesis through a series of switches, some angiogenesis-stimulating growth factors and some angiogenesis inhibitors. When angiogenic growth factors are produced in excess of angiogenesis inhibitors, the balance is tipped in favor of blood vessel growth. When inhibitors are present in excess of stimulators (TAFs), angiogenesis is stopped. The normal, healthy body maintains a perfect balance of angiogenesis modulators. In many serious diseases states, the body looses control over angiogenesis. Angiogenesis-dependent diseases result when new blood vessels either grow excessively or insufficiently. Nowadays angiogenesis is very widespread studied in relation with the growth of tumours.

Tumour-induced angiogenesis is believed to occur when normal tissue vasculature is no longer able to support growth of an avascular tumour. At this stage the tumour cells, lacking nutrients and oxygen, become hypoxic. This is assumed to trigger cellular release of tumour angiogenic factors, TAF, which start to diffuse into the surrounding tissue and approach endothelial cells (EC's) of nearby blood vessels [16]. EC's subsequently respond to the TAF concentration gradients by forming sprouts, dividing and migrating towards the tumour. A summary of these mechanisms can be found in the recent paper by Jain and Carmeliet [17]. Figure 1 shows examples of real or simulated vascular networks.

In developing mathematical models of angiogenesis, the hope is to be able to provide a deeper insight into the underlying mechanisms which cause the process. If the relevant signals could be intercepted through well-targeted drugs and the blood

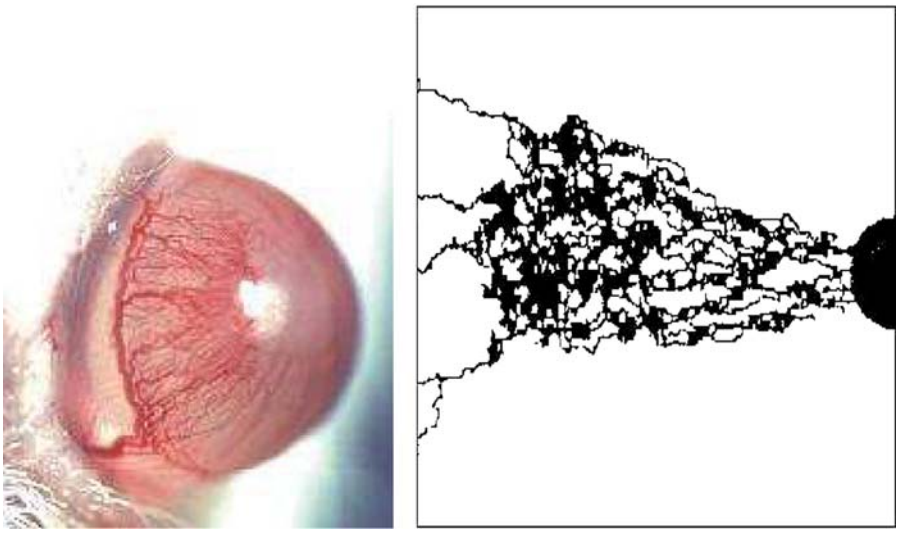

Fig. 1 Angiogenesis on a rat cornea (from [13]) (*left*). A simulation of an angiogenesis due to a localized tumor mass (*black region* on the *right*) (from [11]) (*right*)

supply to cancerous formations thus interrupted, then the tumors themselves might be starved to death, or at least to dormancy [12,15]. These processes and future reparative strategies require a complete understanding of angiogenesis at the capillary level. An important goal would then be the integration of mathematical models for angiogenesis and tumor growth, but the existing unsolved complexity of the individual models has still prevented such an integration.

The angiogenic system is extremely complex, due to its intrinsic multiscale structure; a major source of complexity in the mathematical modelling derives from the strong coupling of the kinetic parameters of the relevant stochastic branching-and-growth of the capillary network at the microscale, with a family of interacting underlying fields at a macroscale. This is the reason why in literature we may find many mathematical models addressing some of the features of the angiogenic process and still the problem of capturing the relevant keys of the process is open.

Our main interest is not in the modelling of the angiogenic phenomenon; in the past two decades, several mathematical models have been proposed. The first one-dimensional continuum models [6,9,19] were based on partial differential equations describing the evolution of macroscopic quantities such as cell density and chemical concentrations. However they were not able to capture some multiple scales characteristics of the phenomenon. Two-dimensional continuum models of angiogenesis [10,22] provided more detailed information for the spatial temporal distribution of capillary sprouts, but are still unable to incorporate certain events such as repeated sprout branching. Consequently, they do not adequately describe the overall dendritic structure of the capillary network. A different approach is given by the Lagrangian description of the capillary networks which provides a tracking of the individual cells moving over time. This approach might be both deterministic or stochastic. A two-dimensional probabilistic model was proposed in the early 1990s; the authors have described the evolution of the velocities of individual endothelial cells by stochastic differential equations [28]. They introduced in the model random motility, chemotaxis, sprout branching and anastomosis so that realistic capillary network structures were produced, but they had not described the interaction between the endothelial cells and the extracellular matrix yet. This interaction has been modelled by Anderson et al. [2,3] by the coupling of a discrete probabilistic model on a regular lattice describing the movement of endothelial cells and continuum equations for the concentration of chemical factors and the extracellular matrix. The discrete models have been derived via a discretisation of the governing continuous equations. Within the framework of the reinforced random walk [14] and its associated master equation, both continuous [18] and regular discrete lattice [23] models have been formulated. In particular in [18] the authors are interested in the mechanism of capillary sprouting from the parental vessel as a result of aggregation of endothelial cells; the movement of cells is taken in the diffusive approximation. In [24], a circular random walk model has been applied to the process of angiogenesis, thus allowing cells to move, independently of each other, on a lattice; the results show good agreement with empirical observations. As stressed by the authors this approach has the advantage of providing a natural link between the microscopic and macroscopic forms. However none of them capture in the continuum model sprout branching, anastomosis, and cell proliferation. All the discrete models mentioned above, but the one in [28], are discrete in time. Furthermore in the models

all the authors refer to the density of endothelial cells. In this way a natural way to track the fibers of the capillary is lost.

The aim of this paper, more than providing additional models, is to propose a novel mathematical approach for reducing complexity by (locally) averaging the stochastic cell, or vessel densities in the evolution equations of the underlying fields, at the mesoscale, while keeping stochasticity at lower scales, possibly at the level of individual cells or vessels [5]. In this way only the simple stochasticity of the geometric processes of birth (branching) and growth is kept, having reduced the local dependence of the relevant kinetic parameters upon deterministic mean underlying fields. This kind of models are known as hybrid models.

A satisfactory mathematical modelling of angiogenesis and of many other fiber processes requires a geometric theory of stochastic fibre processes. As a working example, we present here a simplified stochastic geometric model, largely inspired by current literature, for a spatially distributed angiogenic process, strongly coupled with a set of relevant underlying fields. The branching mechanism of blood vessels is modelled as a stochastic marked counting process describing the birth of new tips, while the network of vessels is modelled as the union of the trajectories developed by tips; consequently capillary extensions are modelled by a system of a random number of Langevin-type stochastic differential equations, coupled with the random PDE's describing the evolution of the underlying fields involved in the process.

The initiation of sprouting from the preexisting parental vessel is not considered here; in order to avoid further mathematical technicalities, we assume a given number N_0 of initial capillary sprouts; we refer to literature [18] for details on this topic. For the time being, we perform a heuristic law of large numbers as the number of tips increases, showing that, when the number of tips, and then of trajectories, is large enough, the model might be described by the mean density of endothelial cells [7,20,21]. Indeed the joint density of position and velocity of cells cannot be explicitly decoupled, so that in the limit we get a partial differential equation for the joint density coupled with the, now deterministic, PDE's describing the evolution of the underlying fields involved in the process. A very similar approach has been recently proposed in [29], though the authors do not consider stochasticity at the microscale, still considering an averaging at the mesoscale. In the modelling and statistical analysis of the mentioned systems it is of great importance to handle random closed sets of different (even though integer) Hausdorff dimensions, usually smaller than the dimension $d \in \mathbb{N}$ of the relevant space. Here the original approach proposed in [1,8] is used, by introducing stochastic generalized densities (distributions) *à la Dirac-Schwartz*, for which mean generalized densities are meaningful. For the applications of our interest, the *Delta formalism* provides a natural framework for deriving evolution equations for mean densities of tips (of Hausdorff dimension 0), and of vessel networks (of Hausdorff dimension 1) in terms of the local relevant kinetic parameters of branching and extension.

It may be of interest for the reader to notice that in [29] mollified versions of such generalized densities have been widely used in the numerical simulations, for bridging the microscale and the macroscale, though their stochastic aspect at the microscale has been ignored. We wish to stress that anyhow substituting mean geometric densities of tips, or of full vessels to the corresponding stochastic quantities leads to an acceptable coefficient of variation (percentage error) only when a law of large numbers can be

applied, i.e. whenever the relevant numbers per unit volume are sufficiently large; otherwise stochasticity cannot be avoided, and in addition to mean values, the mathematical analysis and/or simulations should provide confidence bands for all quantities of interest.

2 The mathematical model

A well-known model in literature is based on the idea that the endothelial cell proliferate and migrate in response to different signalling cues; in particular they move though a gap in the basement membrane and into extra cellular matrix (ECM). They secrete proteolytic enzymes, which also degrade the ECM. Migration is thought to be controlled by chemotaxis, the directed cell movement up the gradient of a diffusible substance, a growth factor emitted by the tumor (here TAF), and by haptotaxis, the directed cell movement along a nondiffusible substance, an adhesive gradient (here fibronectin). TAF and fibronectin bind to specific membrane receptors of endothelial cells, activating cell migration machinery. Then cells produce a matrix degrading enzyme (MDE), which improves the attachment of the cells to fibronectin contained in the extracellular matrix. As a consequence endothelial cells are able to exert the traction forces needed for migration.

2.1 Network dynamics

Based on the above discussion, the main features of the process of formation of a tumour-driven vessel network are

(i) vessel branching;
(ii) vessel extension;
(iii) chemotaxis in response to a generic tumour angiogenetic factor (TAF), released by tumour cells;
(iv) haptotatic migration in response to fibronectin gradient, emerging from the extracellular matrix and through degradation and production by endothelial cells themselves;
(v) anastomosis, when a capillary tip meets an existing vessel.

Modelling the capillary network

Let N_0 denote the initial number of tips, $N(t)$ the numbers of tips at time t, and $X^i(t) \in \mathbb{R}^d$ the location of the i-th tip at time t. We model sprout extension by tracking the trajectory of individual capillary tips. As a consequence,

$$X(t) = \bigcup_{i=1}^{N(t)} \{X^i(s), T_i \leq s \leq t\}$$

will be the network of endothelial cells, i.e. the union of the trajectories of the tips, where T_i is the birth time of the i-th tip, i.e. the time when an existing vessel branches

and the i-th trajectory springs up; and

$$Y(t) = \bigcup_{i=1}^{N(t)} \{X^i(s), \tilde{t}_1 \leq t - s \leq \tilde{t}_2\}$$

is the union of the mature parts of vessels that may branch at time t.

2.1.1 Branching

If we denote by T^n and Y^n the birth time and location, respectively, of the n-th tip, the birth process of new tips can be described in terms of a marked point process, by means of the random measure on $\mathcal{B}_{\mathbb{R}^+ \times \mathbb{R}^d}$

$$\Phi = \sum_n \epsilon_{(T^n, Y^n)}, \tag{1}$$

where $\mathcal{B}_{\mathbb{R}^d}$ is a Borel σ-algebra on $\mathbb{R}^d$. Hence, for any measurable set $A \subseteq \mathcal{B}_{\mathbb{R}^+ \times \mathbb{R}^d}$

$$\Phi(A) := \sum_n \epsilon_{(T^n, Y^n)}(A) = \text{card}\{n : (T^n, Y^n) \in A\} \tag{2}$$

is the random variable which counts those tips which are born in A. By definition $\Phi(\{0\} \times \mathbb{R}^d) = N_0$. The jump process $N(t)$, which counts all tips born up to time t, is then defined by $N(t) = \Phi([0, t] \times \mathbb{R}^d)$. The function $t \mapsto N(t)$ takes values in $N_+ = \{0, 1, 2, \ldots\}$ and is right continuous, nondecreasing and piecewise constant, with jumps of size 1 (simple).

Let us remind here that a (simple) marked point process is characterized by its stochastic intensity, i.e. by the infinitesimal probability of branching per unit time and unit volume, conditional upon the history $\mathcal{F}_{t^-}$ of the whole process up to time t^-, i.e. the family of all possible events which may occur before time t

$$\mu(dt \times dx) = \text{prob}(\Phi(dt \times dx) = 1 | \mathcal{F}_{t^-}). \tag{3}$$

For the sake of notation, from now on, we omit the sign minus.

As mentioned, in literature two kinds of branching have been identified, either from a tip or from a mature vessel (see e.g. [2,24,25]). Here we describe explicitly the branching processes from a mathematical point of view. We considered, as it is always supposed, that the branching rates depend on the field of concentration of TAF.

Tip branching During a time interval $]t, t + dt]$, given a TAF's concentration $C(t, x)$, a birth of a new tip may occur in the volume $]x, x + dx]$ from one of the parental tips $X^i(t)$, $i = 1, ..., N(t)$, with a birth rate per unit of volume given by

$$\alpha_1(t, x) = \alpha_1 \beta_1(C(t, x)) \sum_{i=1}^{N(t)} \delta_{X^i(t)}(x), \tag{4}$$

where β_1 is a nonnegative function in $C_b(\mathbb{R}^d)$. For example $\beta_1(x) = \frac{ax}{1+x}, x \in \mathbb{R}_x$. When a tip located in x branches, the initial value of the state of the new tip $\left(X^{N(t)+1}, v^{N(t)+1}\right) = (x, v_0)$, where v_0 is a nonrandom velocity.

Vessel branching During a time interval $]t, t + dt]$ a new tip birth may occur along $Y(t)$ with rate per unit time and unit volume

$$\alpha_2(t, x) = \alpha_2 \beta_2(C(t, x))\ \delta_{Y(t)}(x) \tag{5}$$

with $\alpha_2 \ll \alpha_1$. Again β_2 is a nonnegative function in $C_b(\mathbb{R}^d)$.

By Eqs. (4) and (5), the stochastic intensity (3) becomes

$$\mu(dt \times dx) = \text{prob}(\Phi(dt \times dx) = 1 | \mathcal{F}_{t^-}) = (\alpha_1(t, x) + \alpha_2(t, x))\, dx\, dt. \tag{6}$$

As a consequence, the probability to have a new tip during the time interval $]t, t + dt]$ is obtained by Eq. (6) integrating over $\mathbb{R}^d$

$$\begin{aligned} \text{prob}\,(N(t + dt) - N(t) = 1 | \mathcal{F}_{t^-}) &= \left(\sum_{i=1}^{N(t)} \alpha_1(t, X^i(t)) + \int_{\mathbb{R}^d} \alpha_2(x, t) dx \right) dt \\ &=: \alpha_N(t) dt. \end{aligned} \tag{7}$$

Now we are also able to give the probabilities to have either a tip (the k-th) or a vessel branching are given by the following expressions. Indeed

$$\text{prob(new birth in }]t, t + dt] \text{ at } X^k(t) | \mathcal{F}_{t^-}) = \frac{\alpha_1(t, X^k(t))}{\alpha_N(t)} dt \tag{8}$$

and

$$\text{prob (new birth in }]t, t + dt] \text{ in }]x, x + dx] \subset Y(t) | \mathcal{F}_{t^-}) = \frac{\alpha_2(t, x)}{\alpha_N(t)} dt dx. \tag{9}$$

2.1.2 Vessel extension

As far as movement (extension) is concerned, we consider a Langevin model

$$\begin{aligned} dX^i(t) &= v^i(t)(1 - p_a \mathbb{I}_{X(t)}(X^k(t)) dt, \quad t > T^i, \\ dv^i(t) &= a(X^i(t), v^i(t), t) dt + \sigma dW^i(t), \quad t > T^i, \end{aligned} \tag{10}$$

where $v^i(t)$ is the velocity of the i-th tip at time t. The drift $a(x, v, t)$ is a function of the concentrations $C(t, x)$ of TAF and $f(x, t)$ of fibronectin and/or their gradients; in particular

$$a(X^i(t), v^i(t), t) = -k v^i(t) + F\left(C(t, X^i(t)), f\left(t, X^i(t)\right)\right), \tag{11}$$

i.e. we consider an inertial component and a bias due to the underlying fields. As in [24,27], we take the bias depending on the TAF and the ficronectin fields

$$F\left(C\left(t, X^i(t)\right), f\left(t, X^i(t)\right)\right) = d_C(C(t, X^i(t)))\ \nabla C(t, X^i(t)) + d_f\left(f\left(t, X^i(t)\right)\right)\ \nabla f\left(t, X^i(t)\right). \quad (12)$$

d_C, d_f, are turning coefficients, modelled as following

$$d_C\left(C(t, X^k(t))\right) = d_1 \frac{\left|\nabla C\left(t, X^k(t)\right)\right|}{(1 + \gamma C(t, X^k(t))^q}, \quad (13)$$

$$d_f\left(f(t, X^k(t))\right) = d_2 \left|\nabla f(t, X^k(t))\right|, \quad (14)$$

where $\gamma, q \geq 0$. So the reorientation of the cells increases as a function of the magnitude of the chemotactic, haptotactic gradient; furthermore cells becomes desensitised to chemotactic gradients at high attractant concentrations, as stressed in [2,18].

In Eq. (10) parameter p_a assumes only the 0 and 1 values; $p_a = 0$ means that no impingement is considered, otherwise, for $p_a = 1$ the phenomenon of anastomosis is taken into account. $\mathbb{I}_{X(t)}$ denotes the indicator function associated with the existing vessel network $X(t)$; whenever a tip is reconnected with an existing vessel its movement stops and a loop is created. This is called tip-vessel anastomosis.

2.2 Modelling the dynamics of underlying fields

As already mentioned, TAF, fibronectin and matrix degrading enzymes (MDE) activate and regulate the migration of endothelial cells. For the biological motivation of the modelling we take into account the remarks in [27].

Chemotactic field TAF diffuses and decreases where endothelial cell are present. We might consider two different models for the time evolution of $C(t, x)$; indeed we may suppose either that the consumption, i.e. the receptor mediated binding, is due to all the cells of the network or that it is due to the new endothelial cells at the tips, only. In the first case the evolution of C would be described by the following partial differential equation in which the consumption at position x is nonzero around the whole network

$$\frac{\partial}{\partial t} C(t, x) = c_1 \delta_A(x) + d_1 \triangle C(t, x) - \eta C(t, x) \frac{1}{N} (\delta_{X(t)} * V_\epsilon)(x); \quad (15)$$

in the latter case the consumption is proportional to the velocity $v^i, i = 1, \ldots,$ of the tips again in a small region of radius ϵ,

$$\frac{\partial}{\partial t} C(t, x) = c_1 \delta_A(x) + d_1 \triangle C(t, x) - \eta C(t, x) \frac{1}{N} \sum_{i=1}^{N(t)} (v^i(t) \delta_{X^i(t)} * V_\epsilon)(x). \quad (16)$$

Parameters $c_1, d_1, \eta \in \mathbb{R}^+$ represent the rate of production of a source located in a region $A \subset \mathbb{R}^d$, modelling e.g. a tumour mass, the diffusivity and the rate of consumption, respectively. We have denoted by $\delta_{X^i(t)}(x)$ the random distribution (Dirac density) localized at the tip $X^i(t)$, for $i = 1, \ldots, N(t)$; and by $\delta_{X(t)}(x)$ the random distribution localized at the whole network $X(t)$; note that $X^i(t)$ is a random closed set of Hausdorff dimension zero, while $X(t)$ is a random closed set of Hausdorff dimension one.

The convolution with the kernel $V_\epsilon(x)$ provides a mollified version of the relevant random distributions. From a mathematical point of view, the use of mollifiers reduces analytical complexity; from a modelling point of views this might correspond to a nonlocal reaction with the relevant modelling fields. It is of interest to notice that according to the theory of stochastic distributions developed in [1,8] the expected value of a Dirac delta's $\delta_{X^i(t)}$ is the probability density distribution of tips (see Sect. 3).

In Eqs. (15)–(16), and later in Eqs. (18)–(19), rescaling by N the reaction terms corresponds to consider a dependence of such terms upon the (mollified) empirical distribution of either the existing vessels in the first case, or the variation in length of the existing vessels, per unit time, in the latter case, according to two different modelling assumptions. Correspondingly, the mollifier kernel V_ϵ is chosen such that $\lim_{\epsilon \to 0} V_\epsilon(x) = \delta_0(x)$. Furthermore, $\epsilon \ll 1/N$, so that also

$$\lim_{N \to \infty} V_\epsilon(x) = \delta_0(x). \tag{17}$$

Later these choices will allow the convergence to corresponding densities, for N tending to infinity, by means of suitable laws of large numbers.

Haptotactic field Fibronectin is known to be attached to the extracellular matrix and does not diffuse [4], thus the equation for fibronectin does not contain any diffusion term. As in [27], degradation of fibronectin, characterized by a coefficient γ, depends on the concentration of MDE, produced by the cells. Hence, the concentration of fibronectin $f(x,t)$ produced by the endothelial cells at the tip evolves as

$$\frac{\partial}{\partial t} f(t,x) = \beta \frac{1}{N} \sum_{i=1}^{N(t)} (\delta_{X^i(t)} * V_\epsilon)(x) - \gamma m(t,x) f(t,x). \tag{18}$$

The MDE, once produced with rate ν_1, diffuses locally with diffusion coefficient ϵ_1, and is spontaneously degraded at a rate ν_2.

$$\frac{\partial}{\partial t} m(t,x) = \epsilon_1 \triangle m(t,x) + \nu_1 \frac{1}{N} \sum_{i=1}^{N(t)} (\delta_{X^i(t)} * V_\epsilon)(x) - \nu_2 m(t,x). \tag{19}$$

Equations (15)–(19) are now random partial differential equations, since the source terms depend upon the stochastic geometric process $X(t)$ of the vessel network. A direct consequence is the stochasticity of the underlying fields, and consequently the stochasticity of the kinetic parameters of birth and growth of vessels (for an overview of the methods adopted in this paper the reader may refer to [26]).

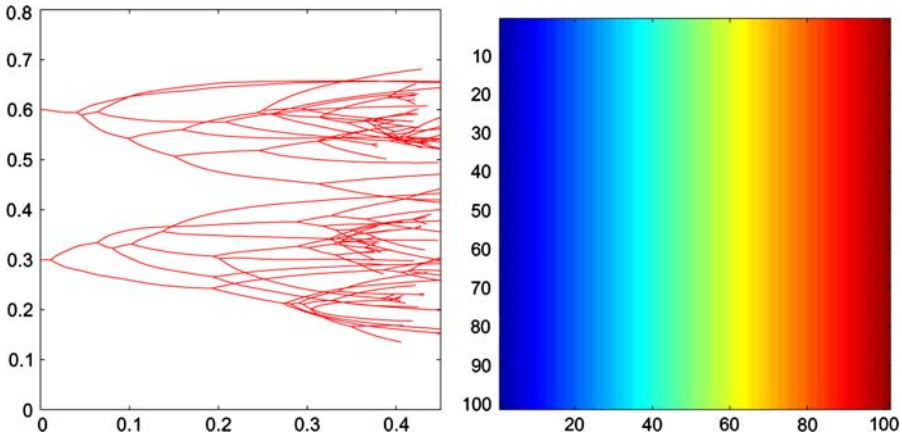

Fig. 2 A vessel network (on the *left*) driven by a constant in time TAF field (on the *right*)

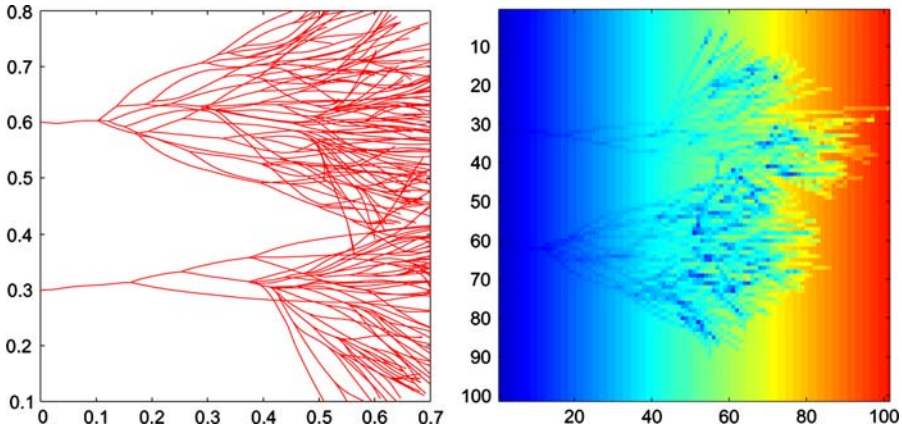

Fig. 3 A vessel network (on the *left*) interacting with a degrading TAF field (on the *right*)

Figures 2 and 3 show the simulation results of System (10)–(14), with $d_2 = 0$, coupled with Eq. (16) in the nonviscous case. In Fig. 2, we have taken a steady-state solution of Eq. (16), while in Fig. 3 also TAF's consumption has been taken into account. As one can see, in the latter case the speed of endothelial cells is lower, and as a consequence much more branches occur. Note that anastomosis has not been considered.

3 The evolution of the tip process

Let us assume for simplicity that $\alpha_2 = 0$, i.e. we consider only the branching of tips. Let us consider System (10)–(14), with $p_a = 0$, coupled with the underlying fields (16)–(19). This means that as this step of the analysis, we do not consider anastomosis.

Here we want to address the problem of the mathematical description of the full stochastic model as time evolves, i.e. as the number of tips (and capillaries) increases.

Let us consider two fundamental random spatial measures, describing the system at time t. Let Q_N be the empirical measure of the processes $(X^k(t), v^k(t)), k = 1, \ldots, N(t)$

$$Q_N(t) = \frac{1}{N} \sum_{i=1}^{N(t)} \epsilon_{(X^k(t), v^k(t))} \tag{20}$$

and $T_N(t)$ be the random empirical distribution of tips

$$T_N(t) = \frac{1}{N} \sum_{i=1}^{N(t)} \epsilon_{X^k(t)} = Q_N(t)(\cdot \times \mathbb{R}^d), \tag{21}$$

where N is a suitable scale parameter. Furthermore we consider the empirical spatial distribution of velocities

$$V_N(t) = \frac{1}{N} \sum_{i=1}^{N(t)} v_k(t) \epsilon_{X^k(t)}. \tag{22}$$

From (20) and (22), we have that for any Borel set B_1 in $\mathbb{R}^d$,

$$V_N(t)(B_1) = \frac{1}{N} \sum_{i=1}^{N(t)} v_k(t) \epsilon_{X^k(t)}(B_1) = \int_{B_1 \times \mathbb{R}^d} v \, Q_N(t)(d(x, v)). \tag{23}$$

Heuristically, if we suppose that $Q_N(t)$ converges to a limit measure $Q_\infty(t)$, absolutely continuous with respect to the usual Lebesgue measure on $\mathbb{R}^d \times \mathbb{R}^d$,

$$Q_\infty(t)(d(x, v)) = p(t, x, v) d(x, v),$$

then we would have limit measures also for $T_N(t)$ and $V_N(t)$, i.e. $T_\infty(t)(dx) = \tilde{p}(t, x)dx$; and $V_\infty(t)(dx) = w(t, x)dx$, where

$$\tilde{p}(t, x) = \int p(t, x, v) dv \tag{24}$$

$$w(t, x) = \int v \, p(t, x, v) dv. \tag{25}$$

This will be the subject of forthcoming theoretical investigations.

Convergence of Q_N

By Itô's formula we may obtain an evolution equation for the measure Q_N.

Let $g \in C_b(\mathbb{R}^d \times \mathbb{R}^d)$. By Itô's formula, from System (10), we get

$$\begin{aligned} d\, g\left(\left(X^k(t), v^k(t)\right)\right) &= d\, g\left(\left(X^k(0), v^k(0)\right)\right) + \nabla_x g\left(\left(X^k(t), v^k(t)\right)\right) dX^k(t) \\ &\quad + \nabla_v g\left(\left(X^k(t), v^k(t)\right)\right) dv^k(t) \\ &\quad + \frac{1}{2}\Delta_v g\left(\left(X^k(t), v^k(t)\right)\right)\left(dv^k(t)\right)^2 \\ &= d\, g\left(\left(X^k(0), v^k(0)\right)\right) + \nabla_x g\left(\left(X^k(t), v^k(t)\right)\right) v^k(t) \\ &\quad - \nabla_v g\left(\left(X^k(t), v^k(t)\right)\right) \\ &\quad \times [k v^k(t) - F\left(C\left(t, X^k(t)\right), f\left(t, X^k(t)\right)\right)]dt \\ &\quad + \frac{\sigma^2}{2}\Delta_v g\left(\left(X^k(t), v^k(t)\right)\right) dt \\ &\quad + \sigma \nabla_v g\left(\left(X^k(t), v^k(t)\right)\right) dW^k(t). \end{aligned} \tag{26}$$

Thanks to Eq. (26) we may obtain evolution equations for the random measure Q_N, as follows. For any $B \in \mathcal{B}_{\mathbb{R}^d \times \mathbb{R}^d}$

$$\begin{aligned} &\int_B g(x,v) Q_N(t) d(x,v) \\ &= \int_B g(x,v) Q_N(0) d(x,v) + \int_0^t \frac{1}{N} \sum_{k=1}^{N(s)} \nabla_x g\left((X^k(s), v^k(s))\right) v^k(s) ds \\ &\quad + \int_0^t \int_B g(x,v) \alpha_1(s,x) Q_N(s)(d(x) \times \{v_0\}) ds \\ &\quad + \int_0^t \frac{1}{N} \sum_{k=1}^{N(s)} \Big[\nabla_v g((X^k(t), v^k(t)))\left[-k v^k(t)\right] + \left[F(C(t, X^k(t)), f(t, X^k(t)))\right] \\ &\quad + \frac{\sigma^2}{2}\Delta_v g\left((X^k(t), v^k(t))\right)\Big] ds + \tilde{M}_N(t) \\ &= \int_B g(x,v) Q_N(0) d(x,v) + \int_0^t \int_B \Big[\nabla_x g(x,v) v + g(x,v)\alpha_1(s,x)\delta_{v_0}(v) \\ &\quad - \nabla_v g(x,v)\left[k v - F\left(C(t,x), f(t,x)\right)\right] \\ &\quad + \frac{\sigma^2}{2}\Delta_v g(x,v)) \Big] Q_N(t)(d(x,v)) ds + \tilde{M}_N(t), \end{aligned} \tag{27}$$

where the last term

$$\tilde{M}_N(t) = \int_0^t \int_{\mathbb{R}^n} [\Phi_N(ds, dx) - N\alpha(s, x)T_N(s)(dx)\, ds] + \int_0^t \frac{\sigma}{2N} \sum_{k=1}^{N(t)} \nabla_v g((X^k(t), v^k(t)))dW^k(t)$$

is a zero mean martingale which vanishes in probability, thanks to Doob's inequality for martngales. So in the limit the explicit stochasticity vanishes and we may consider only averaged quantities.

If, formally, we take $Q_N(t)(d(x, v)) \to Q_\infty(t)(d(x, v)) = p(t, x, v)dxdv$, then

$$\int_B g(x, v)p(t, x, v)dxdv = \int_0^t \int_B p(s, x, v)ds\, dxdv \Big[\frac{\sigma^2}{2} \Delta_v g(x, v) + \nabla_x g(x, v)v + g(x, v)\alpha_1(s, x)\delta_{\{v_0\}}(v) - \nabla_v g(x, v)\,[kv - F\,(C(t, x), f(t, x))] \Big]. \quad (28)$$

Equation (28) may be seen as the weak form of the following partial differential equation for the density $p(t, x, v)$

$$\frac{\partial}{\partial t} p(t, x, v) = -v \cdot \nabla_x p(t, x, v) + k\nabla_v \cdot (vp(t, x, v)) + \alpha_1(t, x)p(t, x, v_0) - \nabla_v \cdot [F\,(C(t, x), f(t, x))\, p(t, x, v)] + \frac{\sigma^2}{2} \Delta_v p(t, x, v). \quad (29)$$

Convergence of the underlying fields As already mentioned, once it is proven that the measure $Q_N(t)$ converges, so will the measures $T_N(t)$ and $V_N(t)$ do, and by Eqs. (24) and (25), we may derive the following deterministic equations for the relevant underlying fields

$$\begin{aligned} \frac{\partial}{\partial t} C(t, x) &= c_1\delta_A(x) + d_1 \triangle C(t, x) - \eta C(t, x)w(t, x). \\ \frac{\partial}{\partial t} f(t, x) &= \beta \tilde{p}(x, t) - \gamma m(x, t) f(t, x); \\ \frac{\partial}{\partial t} m(t, x) &= \epsilon_1 \triangle m(t, x) + \nu_1 \tilde{p}(x, t) - \nu_2 m(t, x). \end{aligned} \quad (30)$$

If, instead, we adopt model (15) for C, we should expect that Eq. (30) becomes

$$\frac{\partial}{\partial t} C(t, x) = c_1\delta_A(x) + d_1 \triangle C(t, x) - \eta C(t, x)\lambda(x, t),$$

where $\lambda(x,t) = E(\delta_{X(t)}(x))$ is the mean vessel density [8,29]; this is left to subsequent investigation.

Acknowledgments It is a great pleasure to acknowledge fruitful discussions with Elisabetta Dejana of the Institute FIRC of Molecular Oncology, Stefano Paveri-Fontana and Alessandra Micheletti of the Department of Mathematics of the University of Milano.

References

1. Ambrosio, L., Capasso, V., Villa, E.: On the approximation of geometric densities of random closed sets. RICAM Report N. 2006-14, Linz, Austria (2006)
2. Anderson, A.R.A., Chaplain, M.A.J.: Continuous and discrete mathematical models of tumour-induced angiogenesis. Bull. Math. Biol. **60**, 857900 (1998)
3. Anderson, A.R.A., Chaplain, M.A.J., Newman, E.L., Steele, R.J.C., Thompson, A.M.: Mathematical modelling of tumour invasion and metastasis. J. Theor. Med. **2**, 129154 (2000)
4. Birdwell, C., Brasier, A., Taylor, L.: Two-dimensional peptide mapping of fibronectin from bovine aortic endothelial cells and bovine plasma. Biochem. Biophys. Res. Commun. **97**, 574581 (1980)
5. Burger, M., Capasso, V., Pizzocchero, L: Mesoscale averaging of nucleation and growth models. Multiscale Model Simul. SIAM Interdiscip. J. **5**, 564–592 (2006)
6. Byrne, H., Chaplain, M.: Mathematical models for tumour angiogenesis: numerical simulations and nonlinear wave solutions. Bull. Math. Biol. **57**, 461486 (1995)
7. Capasso, V., Morale, D., Salani, C.: Polymer crystallization processes via many particle systems. In: Capasso, V. (ed.) Mathematical Modelling for Polymer Processing: Polymerization, Crystallization, Manufacturing. Springer, Heidelberg (2000)
8. Capasso, V., Villa, E.: On mean densities of inhomogeneous geometric processes arising in material science and medicine. Image Anal. Stereol. **26**, 23–36 (2007)
9. Chaplain, M., Stuart, A.: A model mechanism for the chemotactic response of endothelial cells to tumour angiogenesis factor. IMA J. Math. Appl. Med. Biol. **10**, 149168 (1993)
10. Chaplain, M.: The mathematical modelling of tumour angiogenesis and invasion. Acta Biotheor. **43**, 387402 (1995)
11. Chaplain, M.A.J., Anderson, A.R.A.: Modelling the growth and form of capillary networks. In: Chaplain, M.A.J., et al. (eds.) On Growth and Form: Spatio-temporal Pattern Formation in Biology, Wiley, Chichester (1999)
12. Cooke, R.: Dr. Folkman's War: Angiogenesis and the Struggle to Defeat Cancer. Random House, New York (2001)
13. Corada, M., Zanetta, L., Orsenigo, F., Breviario, F., Lampugnani, M.G., Bernasconi, S., Liao, F., Hicklin, D.J., Bohlen, P., Dejana, E.: A monoclonal antibody to vascular endothelial-cadherin inhibits tumor angiogenesis without side effects on endothelial permeability. Blood **100**, 905–911 (2002)
14. Davis, B.: Reinforced random walk. Probab. Theor. Relat. Fields **84**, 20322 (1990)
15. Folkman, J.: Tumour angiogenesis. Adv. Cancer Res. **19**, 331358 (1974)
16. Folkman, J., Klagsbrun, M.: Angiogenic factors. Science **235**, 442–447 (1987)
17. Jain, R.K., Carmeliet, P.F.: Vessels of Death or Life. Sci. Am. **285**, 38–45 (2001)
18. Levine, H.A., Sleeman, B.D., Nilsen-Hamilton, M.: Mathematical modelling of the onset of capillary formation initiating angiogenesis. J. Math. Biol. **42**, 195238 (2001)
19. Liotta, L., Saidel, G., Kleinerman, J.: Diffusion model of tumor vascularization. Bull. Math. Biol. **39**, 117128 (1977)
20. Morale, D., Capasso, V., Ölschlaeger, K.: An interacting particle system modelling aggregation behavior:from individuals to populations. J. Math. Biol. **50**, 49–66 (2005)
21. Oelschläger, K.: On the derivation of reaction-diffusion equations as limit dynamics of systems of moderately interacting stochastic processes. Probab. Theor. Relat. Fields **82**, 565–586 (1989)
22. Orme, M., Chaplain, M.: A mathematical model of the first steps of tumour-related angiogenesis: capillary sprout formation and secondary branching. IMA J. Math. Appl. Med. **14**, 189205 (1996)
23. Plank, M.J., Sleeman, B.D.: A reinforced random walk model of tumour angiogenesis and anti-angiogenic strategies. IMA J. Math. Med. Biol. **20**, 135181 (2003)

24. Plank, M.J., Sleeman, B.D.: Lattice and non-lattice models of tumour angiogenesis. Bull. Math. Biol. **66**(6), 1785–1819 (2004)
25. McDougall, S.R., Anderson, A.R.A., Chaplain, M.A.J.: Mathematical modelling of dynamic tumour-induced angiogenesis: clinical implications and therapeutic targeting strategies. J. Theor. Biol. **241**, 564–589 (2006)
26. Schweitzer, F.: Brownian Agents and Active Particles. Springer, Heidelberg (2003)
27. Stéphanou, A., McDougall, S.R., Anderson, A.R.A., Chaplain, M.A.J.: Mathematical modelling of the influence of blood rheological properties upon adaptative tumour-induced angiogenesis. Math. Comput. Model. **44**(1–2), 96–123 (2006)
28. Stokes, C.L., Lauffenburger, D.A.: Analysis of the roles of microvessel endothelial cell random motility and chemotaxis in angiogenesis. J. Theor. Biol. **152**, 377–403 (1991)
29. Sun, S., Wheeler, M.F., Obeyesekere, M., Patrick, C.W. Jr.: A multiscale angiogenesis modeling using mixed finite element methods. SIAM J. Multiscale Model. Simul. **4**(4), 1137–1167 (2005)